Malaysian Journal of Catalysis
http://mjcat.utm.my/

New tungsten-sulphate modified silica-titania as oxidative-acidic bifunctional catalyst for diol formation

Swee Ean Lim[a] and Siew Ling Lee[a,b]*

[a]*Department of Chemistry, Faculty of Science, Universiti Teknologi Malaysia, 81310 Johor Bahru, Malaysia,* [b]*Center for Sustainable Nanomaterials, Ibnu Sina Institute for Scientific and Industrial Research, Universiti Teknologi Malaysia, 81310 Johor Bahru, Malaysia, *Corresponding Author: sllee@ibnusina.utm.my*

Article history :
Received 30 August 2016
Accepted 13 October 2016

GRAPHICAL ABSTRACT

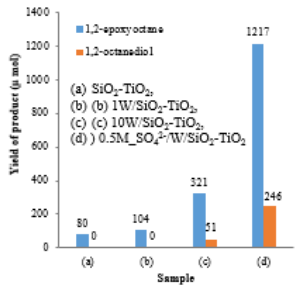

ABSTRACT

A series of new tungsten-sulphate modified silica-titania bifunctional catalysts were successfully synthesized and characterized. The effect of two parameters, namely tungsten oxide loading and sulphuric acid content was studied. SiO_2-TiO_2 was prepared via sol-gel method, followed by impregnation with tungsten oxide (WO_3) and sulphate group (SO_4^{2-}). XRD results demonstrated that monoclinic WO_3 appeared in samples of high tungsten loading. A drastic decrease of ~70% in surface area of solid catalyst from 725.8 to 215.3 m^2/g was observed after loading with both WO_3 and SO_4^{2-}. Existence of both WO_3 and hydrated tetrahedral Ti in the materials was crucial to generate oxidative sites. Further modification with SO_4^{2-} has significantly improved both oxidative ability and acid strength of solid catalyst, producing several folds higher of epoxides and diols. Since Brønsted acid sites are needed for transformation of epoxides to diol, it was believed that the current materials possessed Brønsted acidity. Evidently, the coexistence of WO_3 and SO_4^{2-} were vital to generate both oxidative and acidic sites in SiO_2-TiO_2. The results suggested that 0.5M_SO_4^{2-}/W/SiO_2-TiO_2 was a promising bifunctional catalyst in diol synthesis which yielded 1217 µmol 1,2-epoxyoctane and 246 µmol 1,2-octanediol after 24 h reaction.

Keywords: *Bifunctional catalyst, Oxidative, Acidic, Tungsten oxide, Sulphuric acid*

| eISSN 0128-2581 |

1. INTRODUCTION

In industry, the production of diols is carried out via dual steps reaction. This includes epoxidation of olefin and subsequent hydrolysis of the epoxides. Therefore, the production is carried out in separate chambers with respective oxidative and acidic catalysts. As the process is time-consuming and costly, a bifunctional catalyst which comprises of both catalytic properties in a single material is highly demanded to ensure rapid production of diols.

Several bifunctional oxidative and acidic catalysts have been reported by incorporating different transition metal oxides onto different catalyst support [1-4]. The interaction of transition metal oxides with support material play a role in influencing the type of acidity generated. However, the performance is less satisfactory in terms of amount of Lewis and Brønsted acidity created, selectivity as well as catalytic yield. Theoretically, it was reported that Brønsted acid sites originated from tungsten oxide are one of the strongest among metals [5]. Therefore, the interaction of tungsten oxide and H_2SO_4 with silica-titania in formation of oxidative and acidity sites in a single material is worth to be explored.

In this work, a new series of WO_3 and SO_4^{2-} modified silica-titania bifunctional catalysts were prepared and subsequently characterized. The catalytic performance of the materials were evaluated in the one-step consecutive transformation of 1-octene to 1,2-octanediol via 1,2-epoxyoctane as intermediate.

2. EXPERIMENTAL

2.1 Catalysts Preparation

Silica-titania (mol ratio = 33:1) was synthesized via sol gel method as described elsewhere [6]. A mixture of tetraethylorthosilicate (TEOS, Aldrich, 99.8%), ethanol (EtOH), H_2O and nitric acid (HNO_3) (mol ratio= 1: 1: 4: 0.6) was stirred at room temperature for 30 minutes. Next, a mixture of titanium(IV) isopropoxide (TTIP, Aldrich, 97%), EtOH and acetylacetone (mol ratio= 1: 100: 0.5) was added to the former mixture and stirred under same condition, followed by drying at 80 °C until a clear gel was obtained. The material was dried overnight and subsequently calcined at 500 °C for 5 hours to yield SiO_2-TiO_2 powder.

Wet impregnation method was employed to load tungsten onto prepared SiO_2-TiO_2 powder. For this purpose, ammonium tungstate pentahydrate (AMT, Qrec, 99.9%) was first dissolved in 10 mL of water. The wet impregnated material was stirred vigorously at room temperature for 1 hour, followed by drying overnight and calcination at 500 °C for 5 hours. The synthesized materials were denoted as xW/SiO_2-TiO_2, whereby x = 1 and 10 wt% W. The sample that showed better performance in producing diol was further modified with 0.5 M of H_2SO_4 using similar

approach. The mixture of AMT and H_2SO_4 was wet impregnated onto SiO_2-TiO_2. The resulting material was denoted as 0.5M_SO_4^{2-}/W/ SiO_2-TiO_2.

2.2. Characterization

Powder X-ray diffraction (XRD) was employed for crystallinity determination of the samples by means of a Bruker Advance D8 equipped Siemens 5000 diffractometer with Cu K_α (λ=1.5405Å) radiation. The spectra were collected over 2θ range of 10º to 80º with diffracted monochromatic beam at 40 kV and 40 mA. Diffused reflectance UV spectra were carried out using Perkin Elmer Lambda 900 DRUV/Vis spectrometer. The samples were scanned over the range from 200 to 900 nm. Infrared measurements were performed using a Thermo Scientific Nicolet iS10 FT-IR spectrometer using KBr pellet technique. The spectra were recorded in the region of 400-4000 cm^{-1} using a spectral resolution of 2 cm^{-1}.

The morphology of the synthesized materials were characterized using FESEM JSM-6701F with high resolution at 1 nm (15 kV) and 2.2 nm (1 kV) with the maximum 2 nA probe current. Meanwhile, N_2 physisorption isotherms of synthesized materials were characterized using Thermo Scientific™ Surfer Gas Adsorption Porosimeter at -196 ºC. The samples were degassed at 250 ºC for 12 h under high vacuum before isotherm measurement. In order to estimate the amount and strength of acid sites, Temperature-Programmed Desorption (TPD) of ammonia was performed in a Micromeritics AutoChem II 2920 apparatus. The sample was first fluxed with a He flow at temperature up to 500 ºC, maintained for 1 h at this temperature, and then was allowed to cool down to room temperature and exposed to flowing NH_3 (10% He) for 0.5 h. Subsequently, the system was purged for 0.5 h with helium to eliminate excess NH_3 gas. The temperature of the sample was then raised linearly at 10 ºC/min in He (20 mL/min) from room temperature to 800 ºC. The desorbed NH_3 was monitored by means of a TCD and quantified by comparing the areas under the curve if the respective thermograms with those obtained from previous calibration using known amount of NH_3.

2.3. Catalytic testing

The catalytic performance of the samples was evaluated through the consecutive formation of 1,2-octanediol via transformation of 1,2-epoxyoctane from 1-octene. The reaction mixture containing 1-octene (15 mmol, Merck, 97%), H_2O_2 (30 mmol, Merck, 30%) in acetonitrile (10 mL, Merck, 99.9%) was placed in a round bottom flask equipped with a condenser. The reaction was carried out in an oil bath at 70 ºC for 24 h under stirring condition. The products of the reaction were analyzed on a Shimadzu GC 2014 chromatograph using a HP-5 column (30 m x 0.32 mm i.d., 0.25 μm).

3. RESULTS AND DISCUSSION

SiO_2-TiO_2 synthesized in this work was light and fluffy powder even after calcination at 500 ºC for 5 h. Colour changes were observed in tungsten oxide loaded samples: xW/SiO_2-TiO_2 changed from white to yellow and increase in colour intensity with higher tungsten loading; while 0.5M_SO_4^{2-}/W/SiO_2-TiO_2 appeared in pale green after calcination. The colour change would be a good indication for the presence of W and SO_4^{2-} in the samples upon the modifier loading.

Figure 1 shows the X-ray diffractograms of the synthesized materials. No characteristic peak corresponding to Ti was observed, indicating that TiO_2 presents neither in anatase nor rutile form. The amorphous character of the parent material, SiO_2-TiO_2 might be due to the presence of large amount of amorphous silica (mol ratio Si:Ti= 33:1). After loading with 1 wt% W, the amorphous form remained, indicating well distribution of W onto the support. This could be attributed to the low loading amount of W. With increasing of W loading to 10 wt%, a small peak was observed at 2θ = 23.1º for 10 wt% tungsten. This peak was indexed to monoclinic WO_3 (JCPDS 43-1035). The result demonstrated that crystalline WO_3 appears in samples with high loading amount. Noticeably, the XRD pattern of samples showed only a peak with low intensity. A possible explanation to this is due to the usage of large amount of amorphous silica-titania as support. This may also indicate tungsten species were distributed homogeneously throughout the support material [7]. Similar to sample $1W/SiO_2$-TiO_2, no peak corresponded to WO_3 was detected in the sample treated with H_2SO_4. The results may suggest TiO_2, WO_3 and SO_4^{2-} were well dispersed on the catalyst support.

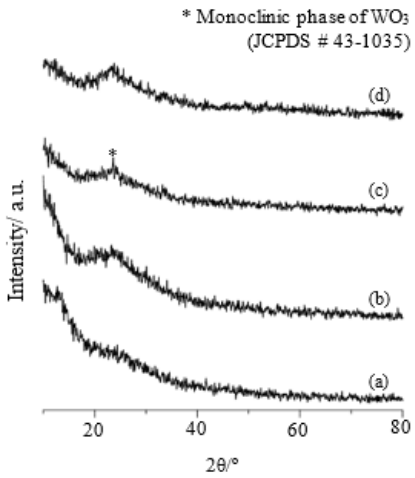

Fig. 1 XRD patterns of (a) SiO_2-TiO_2, (b) $1W/SiO_2$-TiO_2, (c) $10W/SiO_2$-TiO_2 and (d) 0.5M_SO_4^{2-}/W/SiO_2-TiO_2

Figure 2 shows the DR UV-Vis spectra of the samples. As indicated in the Figure 2, there was only a major peak at around 270 nm for SiO_2-TiO_2, which is associated with tetrahedrally coordinated Ti^{4+} species. Indeed, hydrated

tetrahedral Ti^{4+} species is widely acknowledged as the most important Ti species to provide active site for oxidation reaction. This electronic transition was assigned to a charge transfer of tetrahedral Ti sites between O^{2-} and the central Ti(IV) atom [4]. Meanwhile, the peak observed at around 300 nm was linked to the creation of octahedral or polymeric Ti species. A possible explanation to this is some tetrahedral Ti frameworks were transformed into octahedral structure after impregnating with tungsten oxide. The intensity of this peak increased with higher loading of tungsten. The broad band at around 400 nm as observed in materials modified with tungsten oxide was associated to $O^{2-} \rightarrow W^{6+}$ charge transfer transition, as in the case of monoclinic WO_3 [8]. Since the intensity of this peak increased with the increased in tungsten loading, this might indicate more monoclinic WO_3 present in the samples. This also explains the appearance of pale yellow colour of the samples. On the other hand, the bands at 320 and 370 nm were observed in H_2SO_4 impregnated sample. Possibly, the existence of the bands at both 320 and 370 nm was due to the interaction of SO_4^{2-} with WO_3, causing a bathochromic and hypsochromic shifts at 300 and 400 nm, respectively as compared to the samples impregnated with WO_3 alone.

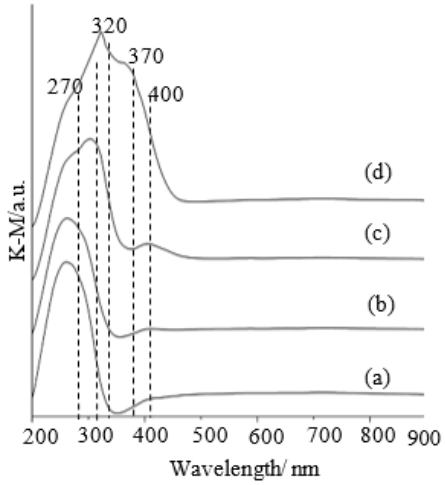

Fig. 2 DR UV-Vis spectra of (a) SiO_2-TiO_2, (b) 1W/ SiO_2-TiO_2, (c) 10W/SiO_2-TiO_2 and (d) 0.5M_SO_4^{2-}/W/SiO_2-TiO_2

FTIR spectra of samples as illustrated in Figure 3 showed typical silicate absorptions at 466 and 1100 cm^{-1} [9]. These bands were associated to Si-O-Si bending and stretching vibrations respectively. The peak at 799 cm^{-1} corresponded to Si-O-Ti or Si-O-W bond, which also associated to tetrahedral Ti. Meanwhile, the peak at 970 cm^{-1} was linked to surface Si-OH vibrations and possibly overlaps absorptions of Si-O-Ti bond [10]. Apart from that, a broad band at 3450 cm^{-1} and a small peak at 1650 cm^{-1} were attributed to stretching and bending frequency of hydroxyl groups respectively. As observed, the intensity of these two bands increased with the increase of WO_3 content in the sample. This implies higher loading of WO_3 enhanced hydrophilicity property of the resulted materials. Surprisingly, no typical band of W=O (ν = 940 cm^{-1}) or O-W-O (ν = 756 cm^{-1}) [11] was observed. Possibly, these bands were overshadowed by Si-OH and Si-O-Ti stretching frequency. Another reason that contributed to such observation is the low amount of WO_3 present in the material as evidenced from XRD analysis. For instance, no bands associated to H_2SO_4 were observed in 0.5M_SO_4^{2-}/W/SiO_2-TiO_2. This could be attributed to the low concentration of H_2SO_4 used during the impregnation process.

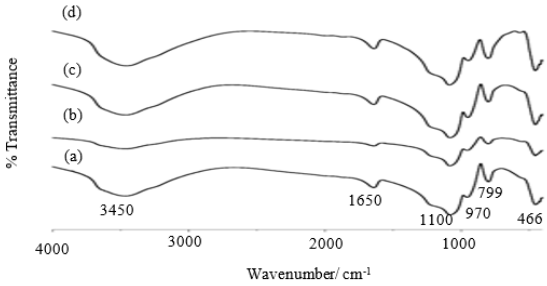

Fig. 3 FTIR spectra of (a) SiO_2-TiO_2, (b) 1W/ SiO_2-TiO_2, (c) 10W/SiO_2-TiO_2 and (d) 0.5M_SO_4^{2-}/W/SiO_2-TiO_2

Surface morphology of the samples was examined using FESEM. Figure 4 shows the FESEM images while Table 1 summarizes the particle size of the samples. Apparently, the surface morphology of the synthesized samples appeared to be coarse and bulky due to agglomeration as observed as in Figure 4 (a). Particles of this material agglomerated with particle size ranged 62-92 nm and a mean of 78 nm. As indicated in Figure 4 (b), the FESEM images of 10W/SiO_2-TiO_2 also displayed agglomeration. On the contrary, the material seemed to be smoother as compared to SiO_2-TiO_2. The particles size of 10W/SiO_2-TiO_2 was in the range 50-80 nm with a mean of 64 nm. An inference that can be drawn from this observation is the particle size experience a slight decrease upon tungsten loading. Similar to previous samples, the particles of 0.5M_SO_4^{2-}/W/SiO_2-TiO_2 displayed agglomeration as indicated in Figure 4 (c). However, the sample appeared to be more compact. The particle size of this material ranged 25-58 nm with a mean of 38 nm. As compared to the parent material and sample modified solely with WO_3, the particle size decreased extensively after impregnation with H_2SO_4. Hence, it can be inferred that modification with both WO_3 and H_2SO_4 has affected the particle size drastically, where the particle growth was stunted.

Table 1 Particle size of SiO_2-TiO_2, 10W/SiO_2-TiO_2 and 0.5M_SO_4^{2-}/W/SiO_2-TiO_2

Samples	Range of particle size	Average particle size
SiO_2-TiO_2	62-92	78
10W/SiO_2-TiO_2	50-80	64
0.5M_SO_4^{2-}/W/SiO_2-TiO_2	25-58	38

Table 2 shows the atomic percentage of all the elements present in the samples. The presence of W in tungsten oxide impregnated sample was confirmed in

addition to TiO_2 and SiO_2 for 10W/SiO_2-TiO_2. As for 0.5M_SO_4^{2-}/W/SiO_2-TiO_2, the presence of W and S was verified. However, the results might not reflect the actual composition of atom since oxygen was taken into account during EDX measurement. This is because the detection of a light element (oxygen) is difficult and quantitatively uncertain. Moreover, the signals of O and Ti intersect, and this can lead to calculative error. In fact, it is well noted that some of the elements might be loss in the process of impregnation.

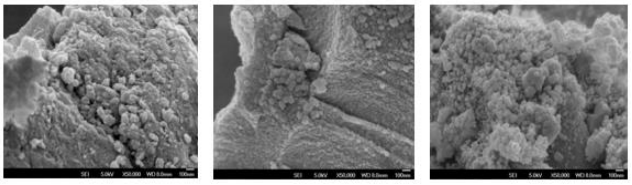

Fig. 4 FESEM micrographs of (a) SiO_2-TiO_2, (b) 10W/SiO_2-TiO_2 and (c) 0.5M_SO_4^{2-}/W/SiO_2-TiO_2 with magnification of 50,000x

Table 2 Elemental analysis using EDX on SiO_2-TiO_2, 10W/SiO_2-TiO_2 and 0.5M_SO_4^{2-}/W/SiO_2-TiO_2

Samples	Atomic Percentage, %				
	Si	Ti	O	W	S
SiO_2-TiO_2	85.01	4.23	7.77	-	-
10W/SiO_2-TiO_2	57.41	1.04	10.27	31.27	-
0.5M_SO_4^{2-}/W/SiO_2-TiO_2	82.48	5.10	9.80	1.93	0.70

Table 3 shows the surface area, pore volume and average pore size of SiO_2-TiO_2, 10W/SiO_2-TiO_2 and 0.5M_SO_4^{2-}/W/SiO_2-TiO_2. As compared to the parent material, 10W/SiO_2-TiO_2 has a surface area of 413.4 m^2/g and pore volume of 0.0702 cm^3/g. The significant decrease in surface area and pore volume might be linked to the deposition of tungsten species inside the pore orifice and formation of crystalline WO_3 on the catalyst surface [7]. As such, obstruction of pores occurred, leading to disruption of pore structure. However, there is no significant change in average pore size after impregnation with tungsten oxide. A slight increase in average pore size of about 3% was observed. A possible explanation to this is the impregnation with tungsten oxide selectively closing the smaller pores, leaving the larger ones for physisorption with N_2. This phenomenon occurred due to the confinement effect.

Table 3 Surface area, pore volume and average pore size of SiO_2-TiO_2, 10W/SiO_2-TiO_2 and 0.5M_SO_4^{2-}/W/SiO_2-TiO_2

Samples	Surface Area (m^2/g)	Pore volume (cm^3/g)	Average pore size (nm)
SiO_2-TiO_2	725.8	0.0998	1.836
10W/SiO_2-TiO_2	413.4	0.0702	1.907
0.5M_SO_4^{2-}/W/SiO_2-TiO_2	215.3	0.1895	1.967

As compared to the parent material, there was a drastic decrease of ~70% in surface area after loading with both WO_3 and SO_4^{2-}. This finding agrees with Lee *et al.* [3] that reported the loading of sulphate group has given a great impact to the surface area of silica-titania aerogel. It was suggested that the decrease of surface area could be due to an agglomeration process in the presence of acid during calcinations. Surprisingly, the pore volume increased slightly (~7%) upon loading with both W and SO_4^{2-}. Possibly, the presence of tungsten during impregnation process has changed the ionic strength of the gel, giving rise to bigger pores as well as a lower surface area [12].

Acidic properties of synthesized materials were determined using NH_3-TPD. Table 4 gives the amount of desorbed NH_3 at various maximum temperatures. The desorption at relatively low temperature region (96.3-109.3 ºC) might be attributed to the desorption of weakly bound ammonia. The concentration of these sites was found to be of no catalytic importance [13]. The intensity of the peak at low temperature region is neither correlated with the number of weak acid sites nor with the catalytic activity of active sites. Meanwhile, the desorption in the high temperature region can be attributed to desorption of NH_3 from strong acid sites which are of catalytic importance. Interestingly, the total acid amount of 10W/SiO_2-TiO_2 at high temperature region (674.3-677.9 ºC) was somehow lower than the parent material, SiO_2-TiO_2. In addition, there was also a very small peak at 312.0 ºC as observed on SiO_2-TiO_2. In contrast, the desorption in the high temperature region for 0.5M_SO_4^{2-}/W/SiO_2-TiO_2 shifted significantly towards higher temperature. This implies upon impregnation with both tungsten oxide and sulphuric acid, the acid strength of the material 0.5M_SO_4^{2-}/W/SiO_2-TiO_2 increases remarkably.

Table 4: Acid site density of SiO_2-TiO_2, 10W/SiO_2-TiO_2 and 0.5M_SO_4^{2-}/W/SiO_2-TiO_2 obtained using NH_3-TPD

Samples	Temperature (ºC)	Total acid amount (mmol g^{-1})
SiO_2-TiO_2	96.3	1.2116
	312.0	0.0093
	677.9	0.6702
10W/SiO_2-TiO_2	109.3	1.2567
	674.3	0.1340
0.5M_SO_4^{2-}/W/SiO_2-TiO_2	99.8	0.94540
	705.6	0.36932
	792.8	0.05811

The evaluation of catalytic performance was conducted at 343 K for 24 h through the consecutive transformation of 1-octene to 1,2-octanediol via the formation of 1,2-epoxyoctane using H_2O_2. It has been widely accepted that oxidative sites are required for transformation of 1-octene to 1,2-epoxyoctane, while Brønsted acid sites are needed for further transformation of 1,2-epoxyoctane to 1,2-octanediol. Figure 5 shows the yield of 1,2-epoxyoctane and 1,2-octanediol after 24 h reaction. Traces of 1,2-epoxyoctane and no 1,2-octanediol were detected in SiO_2-TiO_2 synthesized reaction. This implied that Ti served merely as a weak oxidative site for epoxidation. Similarly, no 1,2-octanediol was observed in sample with low tungsten loading (1W/SiO_2-TiO_2). However, there was a slight increase in the yield of 1,2-

epoxyoctane. Upon increasing the amount of tungsten loading, the yield of 1,2-epoxyoctane quadrupled with traces of 1,2-octanediol formed as compared to the parent material. It is well accepted that hydrated tetrahedrally coordinated Ti species serves as the oxidative site for epoxidation. The current results suggested that the loaded WO_3 species might have played a role as oxidative site in addition to Ti^{4+}.

Evidently, sulphate impregnated sample ($0.5M\_SO_4^{2-}/W/SiO_2$-TiO_2) appears to be the best material in producing both epoxy and diol species. After 24 h reaction, a total of 1217 µmol 1,2-epoxyoctane was detected. As such, it can be deduced that the introduction of SO_4^{2-} has strengthened the oxidative active sites in the synthesized materials. For instance, the reaction also yielded a total of 246 µmol 1,2-octanediol, indicating the material has the best acidic properties. It has been reported that the interaction between PO_4^{3-} and Nb_2O_5 was vital in forming Brønsted acidity in silica-titania [4]. Similarly, the co-existence between SO_4^{2-} and WO_3 in present materials is crucial for generating Brønsted acid sites. In view of the fact that Brønsted acid sites play a role in transformation of epoxides to diol, it was believed that the current materials possessed Brønsted acidity.

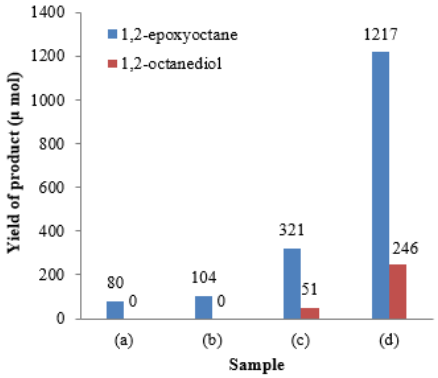

Fig. 5 Catalytic yield of 1,2-epoxyoctane and 1,2-octanediol for (a) SiO_2-TiO_2, (b) $1W/SiO_2$-TiO_2, (c) $10W/SiO_2$-TiO_2, (d)) $0.5M\_SO_4^{2-}/W/SiO_2$-TiO_2

4. CONCLUSION

The synthesis of tungsten-sulphate impregnated silica-titania as oxidative-acidic bifunctional catalyst was performed. From XRD analysis, tungsten oxide appeared as monoclinic WO_3 in samples with higher tungsten loading of 10 wt%. As compared to parent material SiO_2-TiO_2, there was a reduction in particle size, surface area and pore volume in the sample upon impregnation with WO_3. The presence of both hydrated tetrahedral Ti and WO_3 in the materials was crucial to enhance the oxidative ability for producing epoxides. Higher loading of W tended to enhance hydrophilicity of the materials, thereby improving its acidic property. On the other hand, the introduction of SO_4^{2-} has strengthened the oxidative active sites in the synthesized materials, besides generating Brønsted acidity for conversion of epoxides to diol. Evidently, the coexistence of WO_3 and SO_4^{2-} were vital to generate both oxidative and acidic sites in SiO_2-TiO_2. It has been demonstrated that $0.5M\_SO_4^{2-}/W/SiO_2$-TiO_2 appeared a potential oxidative-acidic bifunctional catalyst, producing 1217 µmol 1,2-epoxyoctane and 246 µmol 1,2-octanediol after 24 h reaction.

ACKNOWLEDGEMENT

The authors express gratitude to the Ministry of Higher Education (MOHE), Malaysia and Universiti Teknologi Malaysia for Research University Grants (Q.J130000.2609.10J66 and Q.J130000.2526.13H52).

REFERENCES

[1] D. Prasetyoko, Z. Ramli, S. Endud, H. Nur, J. Mol. Catal., 241(1) (2005a) 118.
[2] D. Prasetyoko, Z. Ramli, S. Endud, H. Nur, Mater. Chem. Phys., 93(2) (2005b). 443.
[3] S. L. Lee, S. C. Wei, H. Nur, H. Hamdan, Int. J. Chem. React. Eng., 8(1) (2010) 1.
[4] J. M. Ekhsan, S. L. Lee, H. Nur, Appl. Catal., A, 471 (2014) 142.
[5] G. Busca, Phys. Chem. Chem. Phys., 1(5) (1999) 723.
[6] L. Yuliati, H. Itoh H. Yoshida, Stud. Surf. Sci. Catal., 162 (2006) 961.
[7] F. Adam, A. Iqbal, Chem. Eng. J., 171(3) (2011) 1379.
[8] G. Ramis, C. Cristiani, A.S. Elmi, P. Villa, G. Busca, J. Mol. Catal., 61(3) (1990) 319.
[9] S.L. Lee, H. Hamdan, J. Non-Cryst. Solids, 354(33) (2008) 3939.
[10] S.L. Lee, H. Nur, P.W. Koh, J.M. Ekhsan, S.C. Wei, *Int. J. Appl. Phys. Math.*, 1(1) (2011) 43.
[11] B. Ingham, S.V. Chong, J.L. Tallon, J. Phys. Chem. B, 109(11) (2005) 4936.
[12] L. Davydov, E.P. Reddy, P. France, P.G. Smirniotis, J. Catal., 203(1) (2001) 157.
[13] M. Niwa, and N. Katada, *Catal. Surv. Asia*, 1(2) (1997) 215.